Phase behavior of krypton and xenon to 50 GPa

Daniel Errandonea,[1,2] Beate Schwager,[1] Reinhard Boehler,[1] and Marvin Ross[3]
[1]*Max Planck Institut für Chemie, Postfach 3060, D-55020 Mainz, Germany*
[2]*HPCAT, Carnegie Institution of Washington, Advanced Photon Source, Building 434E Argonne National Laboratory, 9700 South Cass Avenue, Argonne, Illinois 60439*
[3]*Lawrence Livermore National Laboratory, University of California, Livermore, California 94551*
(Received 6 December 2001; revised manuscript received 6 March 2002; published 13 June 2002)

The fcc-hcp phase transitions of krypton and xenon were investigated using synchrotron angle dispersive x-ray diffraction in a diamond-anvil cell up to 50 GPa. Both gases, heated at the highest pressures, exhibit coexistence of the fcc and hcp phases upon decompression to nearly ambient conditions with a decreasing hcp/fcc ratio.

DOI: 10.1103/PhysRevB.65.214110 PACS number(s): 62.50.+p, 61.50.Ks, 64.70.Kb

I. INTRODUCTION

Previous work on the phase behavior of xenon (Xe) is highly contradictory and very little information is available for krypton (Kr). This lack of accurate data on these simple elements and our previous observation of an unusual decrease in the melting slopes at 20 and 30 GPa (Xe, Kr) motivated us to investigate the phase behavior of these materials at both high pressure and high temperature.

X-ray-diffraction studies suggested that xenon transforms at 14 GPa from the fcc structure to an intermediate close-packed phase and then transforms completely to the hcp structure above 75 GPa.[1] Laser heated diamond-anvil cell (DAC) experiments suggested, however, that a direct, kinetically sluggish fcc-to-hcp transition takes place at 21 GPa.[2] On the other hand, more recently it was reported that the fcc-to-hcp transition occurs martensitically between 3 and 70 GPa without an intermediate phase.[3] Krypton (Kr) also crystallizes in the fcc structure and is predicted to be stable as fcc to 110 GPa.[4] Its room-temperature (RT) equation of state (EOS) was determined by energy-dispersive x-ray techniques up to 55 GPa,[5,6] and by x-ray-absorption spectroscopy measurements up to 30 GPa.[7,8] Polian *et al.* suggested that the fcc structure is probably not stable at very high pressure[6] and Cynn *et al.*, in their study of Xe, mentioned that hcp-like patterns have been observed in Kr at 2.1 GPa.[3] In both rare gases the growing of hcp domains from the fcc structure seems to be related with the observed lowering of the melting temperature from that predicted by the corresponding states theory.[9]

The primary intention of the present work was to check if the coexistence of fcc and hcp phases over a large pressure range is caused by kinetic or nonhydrostatic effects and if the lowering of the melting slope can be explained in terms of a model in which hcp stacking faults act as solutes in a binary system. Ideally, the problem can only be properly addressed by x-ray diffraction at simultaneously high pressure and high temperature. However, such technology has not been available at the time of these studies. We therefore performed high-resolution angle-dispersive synchrotron x-ray-diffraction experiments on temperature-quenched samples in a diamond-anvil cell up to 50 GPa. We observed the coexistence of fcc and hcp in Kr from 50 down to 3.2 GPa and for Xe from 41 down to 1.5 GPa. For both rare gases the EOS was determined. In addition, the fraction of hcp phase as a function of pressure was determined from the relative intensity ratio of hcp(100) and fcc(200), the main peaks inherent to these structures. In Sec. II we briefly review the experimental setup and results and discussions are presented in Sec. III. A preliminary account of the present work was given elsewhere.[10]

II. EXPERIMENTAL DETAILS

The x-ray-diffraction experiments were carried out at the beam line ID30 of the European Synchrotron Radiation Facility. A double Si(111) monochromator was employed to provide an incident energy of 33.16 keV. The focused beam was introduced to the sample through a 20-μm-diameter pinhole. The x-ray-diffraction pattern was recorded on a flat image plate located at a distance of 36 cm from the sample. The images were converted, after removing the saturated peaks, to intensity vs 2θ data using the FIT2D software.[11] Tilt and wavelength/distance corrections were obtained from standard silicon powder images. Indexing, structure solution, and refinements were performed using the GSAS (Ref. 12) and POWDERCELL (Ref. 13) program packages, assuming Lorentzian profiles and considering preferred orientations effects.

The samples were compressed using a DAC with diamond-coated tungsten (W) gaskets. Kr was loaded in the DAC at RT using a 0.3-GPa gas apparatus and Xe was loaded at 0 °C and 50 bars in a gas pressure vessel which was evacuated prior to loading. The gas samples were loaded in two different ways which provide uniform heating of a sample volume which was subsequently x rayed. In the first one (sample 1), a rhenium (Re) heater of 30-μm thickness and approximately 80 μm in diameter with a 30-μm-diameter hole in the center was located inside the gasket hole. This geometry provides nearly uniform heating of the gas sample inside the 30-μm hole of the heater. A schematic view of this high-pressure cell is shown in Fig. 1. In the second one (sample 2), Xe or Kr were trapped in a pressed disc of W (Pt or Fe) powder of 20–30-μm thickness, sandwiched between two thermally insulating 10-μm-thick LiF windows. This arrangement also provided uniform heating of the gas samples of similar dimensions as in case 1. Kr and Xe samples were compressed to 50 and 41 GPa, respec-

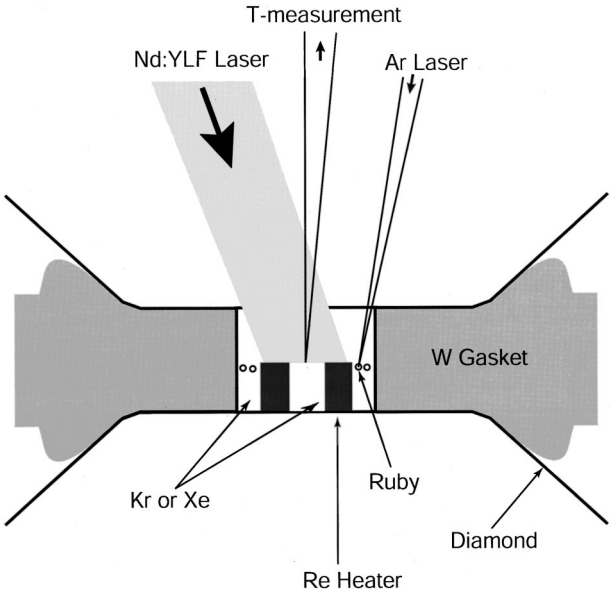

FIG. 1. Schematic description of sample 1. Sample is uniformly heated inside the Re heater, which absorbs the defocused Nd:YLF laser beam. Temperature is measured from a microsized area of the sample and pressure can be measured from unheated ruby chips.

tively, and quenched after laser heating to 2300 K. A 50-W Nd:YLF laser (TEM_{00} mode, $\lambda = 1.053$ μm) was used to heat the samples. X-ray data were collected with decreasing pressure down to nearly ambient conditions. A ruby chip served as a pressure sensor.[14] The pressure obtained in this way is in agreement with that deduced from the Re, W, Fe, and Pt patterns according to the previously established equations of states.[15–17]

III. RESULTS AND DISCUSSION

Figures 2 and 3 show the diffraction spectra measured at different pressures for Kr and Xe, respectively. In all the spectra we have taken, the peaks arising from Re (W, Pt, or

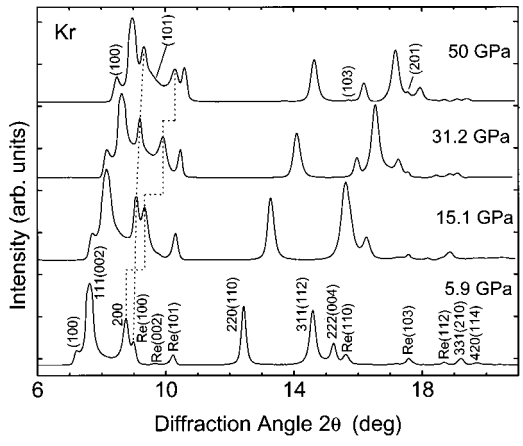

FIG. 2. X-ray-diffraction patterns of Kr at different pressures. Miller indices corresponding to the fcc (hcp) structure are indicated in the lower trace. Re peaks are also labeled. Intrinsic hcp peaks are shown in the upper trace. The different pressure dependence of Re and Kr reflections is also illustrated. The background was removed.

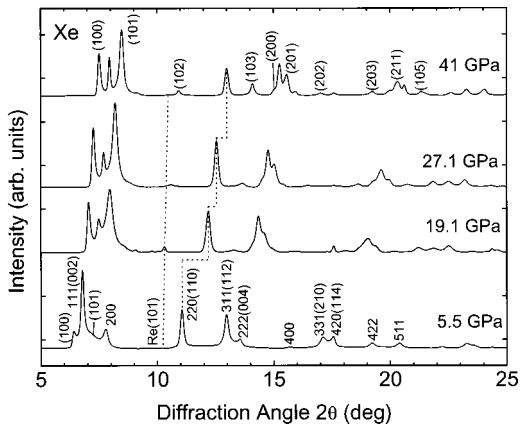

FIG. 3. Same as Fig. 1 but for Xe.

Fe) are easily identified since their pressure shifts are smaller than those of Kr and Xe peaks. The remaining reflections of Kr and Xe patterns can be indexed only on the assumption of the coexistence of fcc and hcp structures. In order to show this more clearly we plot in Fig. 4 the diffraction diagram of a Kr sample at 5.9 GPa together with the refined profile and the individual contribution of the different phases. The deviation from the ideal (111)–(200) intensity ratio observed in Fig. 4 on fcc Kr indicates that some preferred orientation was present. In the refinement shown in Fig. 4 we obtained a low value of the residual for intensities, $R(F^2) = 0.075$, whereas by considering only the presence of a fcc Kr phase the $R(F^2)$ value is significantly larger (0.131). This is also consistently found for all the diffraction patterns of Kr measured above 3.2 GPa and in all the diffraction patterns of Xe collected by us, the reason being that intensities of several reflections cannot be well accounted for without considering the coexistence of both the fcc and hcp structures. This gives quantitive support to the fact that a pressure above about a few giga-

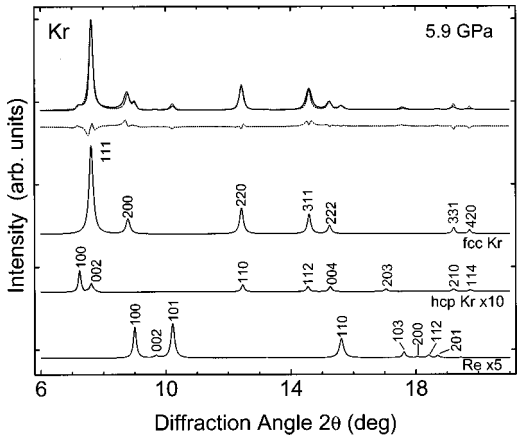

FIG. 4. Diffraction pattern obtained in sample Kr 1 at 5.9 GPa (solid curve, upper trace). The background was removed. The dotted curves represent the fiting curve obtained in the refinement assuming the coexistence of the fcc and hcp phases (upper trace) and the difference between measured data and refined profile (second trace). The three lower traces show the individual contribution of the different phases present. The Re and hcp Kr curves are vertically expanded to better show the presence of weak reflections.

pascals induces the coexistence of the fcc and hcp structures in Xe and Kr.[3]

As shown in Figs. 2 and 3, the positions of some fcc peaks—e.g., (111), (220), (311), and (222)—agree with those of some hcp peaks—e.g., (002), (110), (112), and (004). These correspondences are expected from a disorder in the atomic stacking layers,[3] which seems to be unavoidable in fcc rare-gas solids.[18] In fact, the presence of a high degree of stacking disorder has been reported previously in fcc Kr (Ref. 19) at low temperature. For example, the dhcp structure, another close-packed structure which consists of hexagonal planes with a random stacking order, coexists under freezing at 100 K at ambient pressure with the fcc structure.[19] The coexistence of hcp and fcc phases has been also observed in crystal growth below $0.65T_f$,[20] where T_f is the bulk freezing point. The peaks inherent to the fcc structure are (200), (400), (422), and (511) and the peaks intrinsic to the hcp structure are indicated in the upper traces of Figs. 2 and 3. In both rare gases the intensity of the hcp(100) peak decreases continuously upon decompression, the same trend followed by the hcp(101) peak of Xe. In addition, the rest of the hcp peaks are completely lost below 15 GPa. In contrast with the decreasing of intensity of the intrinsic hcp peaks, the intensity of the intrinsic fcc(200) peak increases when releasing the pressure. All these facts indicate a reduction of the amount of hcp domains present in the sample under decreasing pressure.

In our experiments, the lowest pressure where hcp peaks were observed in Kr was 3.2 GPa, whereas in Xe they were observed even at 1.5 GPa. These values compare well with those reported by Cynn *et al.*[3] for the appearance of the hcp peaks under increasing pressure (2 and 3 GPa, respectively). In the Kr sample studied at 0.9 GPa the hcp peaks had disappeared, but the diffraction peaks corresponding to the fcc structure were still identifiable together with a pronounced broad diffuse scattering, characteristic of the short-range order of liquids. This is in good agreement with the RT liquid-solid transition reported at 0.83 GPa,[21,22] and with the coexistence of crystalline and liquid Kr observed at 0.9 GPa.[23]

It is worthwhile to comment about why the hcp structure was not observed in previous Kr measurements.[5,6] One reason is the higher resolution of our experiments, related to the angle dispersive method and the high brilliance reached in the ESRF. From our results, assuming $2\theta=15°$, it is straightforward to estimate that in an energy dispersive experiment the energy difference between the fcc(100) and the hcp(100) peaks (the highest peak inherent to the hcp structure, see Fig. 4) is about 1 KeV. Then, as the half width of the fcc(100) peak reported by Polian *et al.*[6] is also about 1 KeV, in the energy dispersive experiments the hcp(100) was probably hidden by the fcc(100) peak. The second reason is that after laser heating, the diffraction peaks are sharper and better resolved than those obtained before the laser heating.[3] Because of these facts, it is perhaps not surprising that the coexistence of fcc and hcp phases was not identified in earlier studies, in particular considering that most of the hcp peaks are overlapped by the fcc peaks as explained above. Regarding the x-ray-absorption measurements,[7,8] they give information on the local structure, but cannot distinguish between the fcc and the hcp phases of Kr since both structures have the same number of nearest and second-nearest neighbors with their shells located at the same distances.

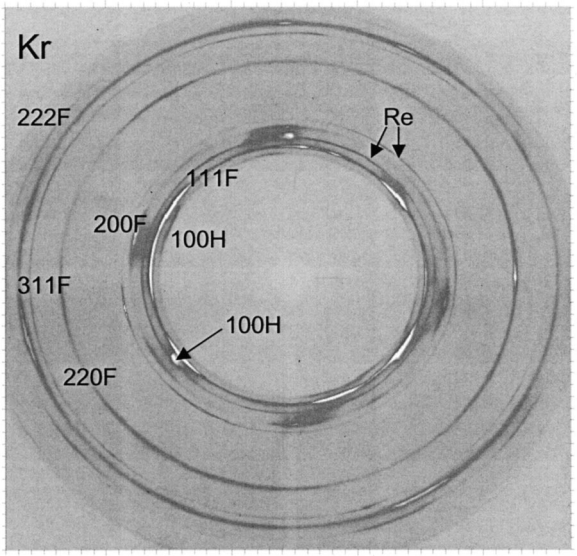

FIG. 5. Debye-Scherrer diffraction rings as recorded on the image plate for Kr at 31.2 GPa, showing the hcp(100) ring and the spots associated to the hcp(101) reflections. *F* and *H* are for fcc and hcp, respectively. Those rings corresponding to both structures (see text) are labeled only as fcc for simplicity. Re indicates the rhenium peaks.

Direct evidence of the observed extra hcp peaks is given in Fig. 5 and 6. Figure 5 shows the Debye-Scherrer diffraction rings of Kr at 31.2 GPa as recorded on the image plate. The inner ring corresponds to the hcp(100) reflections and the spots observed between the fcc(111) and fcc(200) rings (overlapped with one Re ring) correspond to the hcp(101) reflections. Figure 6 shows two image-plate images recorded on Xe at 19.1 GPa (a) and 5.5 GPa (b), respectively, together with their integrated one-dimensional (1D) angle-resolved x-ray-diffraction patterns. At 19.1 GPa the presence of the hcp(100) and hcp(101) rings can be clearly observed, whereas the fcc(200) ring is diffuse. On the contrary, when decreasing the pressure to 5.5 GPa the fcc reflections become more intense and the hcp reflections weaker. The spots and the diffuse scattering observed in both figures were also observed by Cynn *et al.*[3] in Kr and Xe as well as in other systems[24–26] for martensitic fcc-hcp transitions.

In order to get some insight on the fcc-hcp transformation, it is convenient to classify the close-packed structures according to the way the plane hexagonal arrays of atoms are stacked. fcc stacking is characterized by the sequence ABCABC and hcp by the sequence ABABAB. By omitting a layer from the fcc sequence the fcc lattice may have locally small domains ordered in an hcp structure. Since the free-energy difference between fcc and hcp phases is small ($\Delta E < 1$ mRy/atom) and decreases under pressure,[27,28] it is reasonable to expect that thermal fluctuations will occasionally slide the position of an fcc plane to an hcp arrangement.

The intergrowth of hcp domains within an fcc structure has been observed in several systems[24–26] as being always

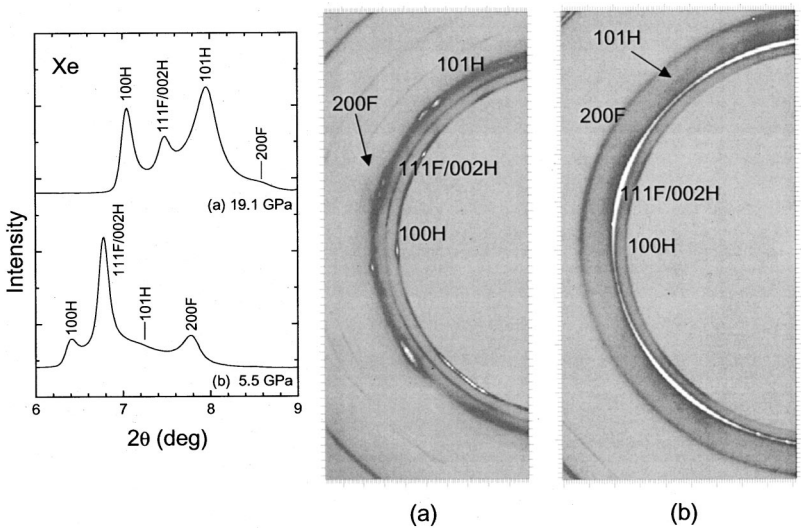

FIG. 6. Angle dispresive x-ray-diffraction patterns of Xe at 19.1 GPa (a) and 5.5 GPa (b). These patterns show the decrease of the intensity of the hcp rings when releasing pressure. *F* and *H* are for fcc and hcp, respectively.

attributed to the developing of stacking disorders. In cobalt, this occurs during the fcc-to-hcp transformation upon cooling at ambient pressure[24] and during compression at room temperature;[25] these two phenomena are apparently related. In Kr and Xe, the fcc-hcp coexistence occurs when they both crystallize below $0.65T_f$ at ambient pressure, while above this temperature only the fcc structure exists.[20] Because of the similarities among the transformation observed upon warming at ambient pressure[20] and the reduction of the hcp/fcc ratio that we have observed under decompression at room temperature with those phenomena observed in cobalt, it is reasonable to assume that, as it happens in cobalt, in Kr and Xe both phenomena are closely related. The possible connection between them seems to indicate that the beginning of growing of the hcp domains may shift toward higher pressures at higher temperatures. This suggestion is coherent with observation by Yoo[29] that the intergrowth of fcc and bcc phases begins at higher pressure with increasing temperature. It gives also additional support to the idea that the considerable decrease observed in the melting slope of Kr and Xe is a consequence of the appearance of hcp domains in their fcc structure,[9] since these unusual changes of the melting slope take place around 2500 K and 30 GPa in Kr and 2700 K and 20 GPa in Xe.[9]

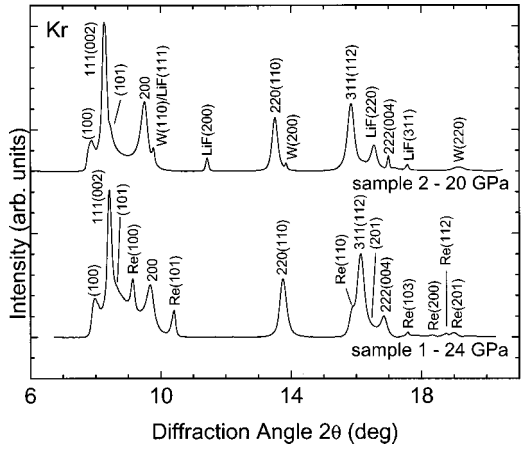

FIG. 7. X-ray-diffraction patterns of samples 1 and 2 of Kr at 24 GPa and 20 GPa, respectively. Miller indices corresponding to the fcc (hcp) structure are indicated in the lower trace. Re, W, and LiF peaks are also labeled. The background was removed.

As the martensitic character of the fcc-hcp transformation seems to be related to the nonhydrostatic conditions of the experiments[3] we decided to study samples 1 and 2 under different conditions as described in the experimental section. We observed a similar behavior in both samples. Figure 7 shows the diffraction pattern obtained for sample 1 of Kr at 24 GPa and sample 2 of Kr at 20 GPa. The intensities of all Kr lines are comparable in both patterns. The same behavior was observed in the Xe samples. It is interesting to see that during laser heating, sample 2 of Kr was molten and sample 1 was not. All these facts indicate that the occurrence of the

TABLE I. Relative volume difference, c/a ratio of the hcp lattice parameters and hcp/fcc ratio as a function of pressure.

P (GPa)	Sample	$(V_{fcc}-V_{hcp})/V_{fcc}$ $(\times 10^{-3})$	c/a	$I_h/(I_h+I_f)$
0.9	Kr 1			
3.2	Kr 2	2.37	1.635	0.02(2)
5.9	Kr 1	7.76	1.639	0.06(3)
15.1	Kr 1	10.55	1.641	0.15(2)
20	Kr 2	13.44	1.640	0.15(5)
24	Kr 1	10.27	1.641	0.12(3)
31.2	Kr 1	8.55	1.640	0.28(5)
40.4	Kr 1	8.01	1.637	0.22(4)
50	Kr 1	5.22	1.638	0.31(5)
1.5	Xe 1	3.87	1.651	0.01(1)
5.5	Xe 1	6.91	1.651	0.29(11)
13.9	Xe 1	4.83	1.672	0.87(17)
19.1	Xe 1	13.04	1.648	0.97(19)
27.1	Xe 1	13.05	1.645	0.97(15)
29	Xe 2	0.43	1.633	0.09(9)
36.2	Xe 2	4.69	1.622	0.98(16)
41	Xe 1	1.14	1.633	0.97(14)

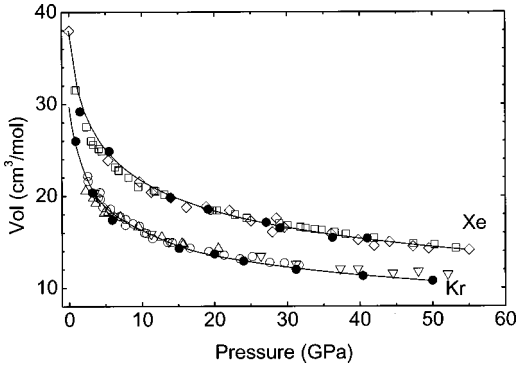

FIG. 8. Comparison of volume data as a function of pressure. Current measurements (●), best fits (——), Ref. 3 (◇), Ref. 5 (▽), Ref. 6 (○), Ref. 7 (△), and Ref. 30 (□). Uncertainties in our data are smaller than the symbols size.

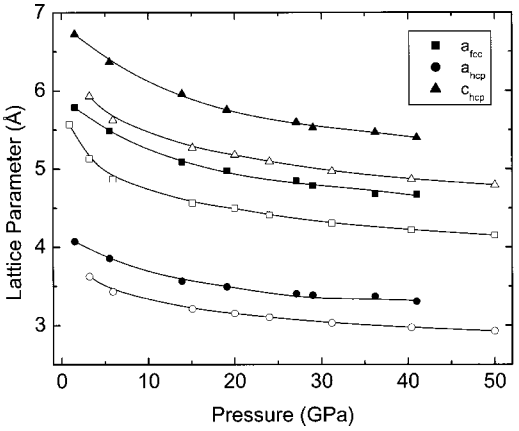

FIG. 9. Pressure dependence of the unit-cell parameters of the fcc (a) and hcp (a) and (c) structure of Kr (empty symbols) and Xe (solid symbols). Lines are to guide the eye.

continuous transition from fcc to hcp is not affected by different run conditions, being mostly induced by the nominal pressure (normal stress).

Volume data for Kr and Xe were obtained for both phases at all the pressures where they are present being the relative difference (shown in Table I) similar to our accuracy in determining the volume (the relative error is $<10^{-2}$). This is not surprising since by modifying the sequence of planes only small atomic displacements are induced (as can be seen in the fact that both structures have identical first- and second-neighbor coordination shells) and thus the transition occurs without a measurable volume change. The pressure dependence of the volumes is plotted in Fig. 8 (only for the fcc structure of Kr and Xe) together with earlier results.[3,5–7,30] The agreement is quite good, but above 30 GPa our Kr data show systematically lower volumes than those of Aleksandrov *et al.*[5] This is not surprising since the accuracy in determining the volume in Aleksandrov measurements was 3%. The fact that both phases have the same volume is reflected in the pressure dependence of the unit-cell parameters, given in Fig. 9. Both the fcc and the hcp unit-cell parameters have the same pressure dependence. This is not surprising since fcc and hcp can be thought of as being polytypes of the same close-packed structure.[31] The Birch-Murnaghan third-order equation fits to our data yield $B_0=2.7(\pm 0.9)$ GPa, $B_0'=5.4(\pm 0.7)$, and $V_0=29.7$ cm^3/mol for Kr and $B_0=4.3(\pm 0.6)$ GPa, $B_0'=5.7(\pm 0.5)$, and $V_0=37.6$ cm^3/mol for Xe, in good agreement with previous results.[3,6,28] Values for V_0 were obtained by extrapolating the high-pressure data to ambient conditions.

It is important to point out that in the hcp phase of Kr and Xe the c/a ratio remains nearly constant under compression, and very close to the ideal value 1.633 (see Table I). This indicates that the compressibility of both axes should be the same and rule out the existence of any intermediate close-packed phase progressing from fcc to hcp by means of shear deformations,[1] giving additional support to the idea that fcc converts to hcp due to the presence of stacking disorders.

Finally, we estimated the relative proportions of fcc and hcp in Kr and Xe from $I_h/(I_f+I_h)$, where I_f and I_h are the integrated area of the fcc(200) and hcp(100) peaks, respectively. We chose these two peaks since they are the main inherent peaks to each structure. The estimates are shown in Table I, where it can be seen that the hcp/fcc ratio increases under pressure, reaching a value close to 0.3 at 50 GPa in Kr and larger than 0.9 at 19.1 GPa in Xe. This ratio might depend on the pressure path of the sample,[3] however, the observed trend suggests that the hcp phase continuously evolves from the fcc phase. This is coherent with the increasing stacking disorders probability[9] due to the decrease in the energy separating the fcc and hcp phases occurring under increasing pressure.[9,27,28] In addition, the smaller increase of the hcp/fcc ratio observed in Kr indicates that the phase transformation might conclude at higher pressures in Kr than in Xe.

In summary, we studied solid Kr and solid Xe by means of an angle dispersive technique up to 50 GPa. We found that in Kr (Xe) upon decompression the fcc and hcp-phases coexist from 50 GPa (41 GPa) to 3.2 GPa (1.5 GPa). The same kind of behavior was previously observed in Xe,[3] suggesting that the fcc-hcp martensitic transition could be a common behavior in all rare-gas solids.

ACKNOWLEDGMENTS

We thank M. Mezouar for technical advice on the beam line ID30 at ESRF and R. Ditz for assistance in sample loading. The present work has been done under Proposal No. HS-1359 at ESRF.

[1] A. P. Jephcoat, H. K. Mao, L. W. Finger, D. E. Cox, R. J. Hemley, and C. S. Zha, Phys. Rev. Lett. **59**, 2670 (1987).
[2] W. A. Caldwell, J. H. Nguyen, B. G. Pfrommer, F. Mauri, S. G. Louie, and R. Jeanloz, Science **277**, 930 (1997).
[3] H. Cynn, C. S. Yoo, B. Baer, V. Iota-Herbei, A. K. McMahan, M. Nicol, and S. Carlson, Phys. Rev. Lett. **86**, 4552 (2001).
[4] D. Young, *Phase Diagram of the Elements* (University of California Press, Berkeley, 1991).
[5] I. V. Aleksandrov, A. N. Zisman, and S. M. Stishov, Zh. Eksp. Teor. Fiz. **92**, 657 (1987) [Sov. Phys. JETP **92**, 657 (1987)].
[6] A. Polian, J. M. Besson, M. Grimsditch, and W. A. Grosshans, Phys. Rev. B **39**, 1332 (1989).
[7] A. Polian, J. P. Itie, E. Dartyge, A. Fontaine, and G. Tourillon, Phys. Rev. B **39**, 3369 (1989).
[8] A. Di Cicco, A. Filipponi, J. P. Itie, and A. Polian, Phys. Rev. B **54**, 9086 (1996).
[9] R. Boehler, M. Ross, P. Soderlind, and D. B. Boercker, Phys. Rev. Lett. **86**, 5731 (2001).
[10] D. Errandonea, B. Schwager, and R. Boehler, High Press. Res. **22**, 75 (2002).
[11] A. P. Hammersley, S. O. Svensson, M. Hanfland, A. N. Fitch, and D. Häusermann, High Press. Res. **14**, 235 (1996).
[12] A. C. Larson and R. B. Von Dreele, Los Alamos National Laboratory Report No. LAUR 86-748, 1994 (unpublished).
[13] W. Kraus and G. Nolze, J. Appl. Crystallogr. **29**, 301 (1996).
[14] H. K. Mao, J. Xu, and P. M. Bell, J. Geophys. Res. **91**, 4673 (1986).
[15] A. L. Ruoff, H. Xia, and Q. Xia, Rev. Sci. Instrum. **63**, 4342 (1992).
[16] Y. K. Vohra, S. J. Duclos, K. E. Brister, and A. L. Ruof, Phys. Rev. Lett. **61**, 574 (1988).
[17] R. Jeanloz, B. K. Godwal, and C. Meade, Nature (London) **349**, 687 (1991).
[18] B. W. van de Waal, Phys. Rev. Lett. **67**, 3263 (1991).
[19] D. W. Brown, P. E. Sokol, and S. N. Ehrlich, Phys. Rev. Lett. **81**, 1019 (1998).
[20] Y. Sonnenblick, Z. H. Kalman, and I. T. Steinberger, J. Cryst. Growth **58**, 143 (1982).
[21] P. H. Lahr and W. G. Eversole, J. Chem. Eng. Data **7**, 42 (1962).
[22] R. K. Crawford and C. A. Swenson, J. Phys. Chem. Solids **36**, 145 (1975).
[23] H. Shimizu, N. Saitoh, and S. Sasaki, Phys. Rev. B **57**, 230 (1998).
[24] F. Frey and H. Boysen, Acta Crystallogr., Sect. A: Cryst. Phys., Diffr., Theor. Gen. Crystallogr. **A37**, 819 (1981).
[25] C. S. Yoo, H. Cynn, P. Soderlind, and V. Iota, Phys. Rev. Lett. **84**, 4132 (2000).
[26] P. S. Kotval and R. W. K. Honeycombe, Acta Metall. **16**, 597 (1968).
[27] I. Kwon, L. A. Collins, J. D. Kress, and N. Troullier, Phys. Rev. B **52**, 15 165 (1995).
[28] P. Sonderlind, J. A. Moriarty, and J. M. Wills, Phys. Rev. B **53**, 14 063 (1986).
[29] C. S. Yoo (private communication).
[30] A. N. Zisman, I. V. Aleksandrov, and S. M. Stishov, Phys. Rev. B **32**, 484 (1985).
[31] C. A. Kittel, *Introduction to Solid State Physics* (John Wiley & Sons, New York, 1996).